CANCER DIAGNOSIS & PROGNOSIS *5*: 300-312 (2025)
doi: 10.21873/cdp.10442

# Dosimetric Comparison of Coplanar, Non-coplanar, and Mixed-Arc VMAT for Head and Face Skin Cancers: A Multi-scenario Analysis

VALENTINA ZAGARDO[1], DENIS LA FAUCI[1], GIUSEPPE EMMANUELE UMANA[2,3], SALVATORE LAVALLE[3], PAOLO PALMISCIANO[4], MANFREDI NOTO[5], ANDREA BONCORAGLIO[6], GIANLUCA SCALIA[3,7] and GIANLUCA FERINI[1,3]

[1]Department of Radiation Oncology, REM Radioterapia srl, Viagrande, Italy;
[2]Department of Neurosurgery, Trauma Center, Gamma Knife Center, Cannizzaro Hospital, Catania, Italy;
[3]Department of Medicine and Surgery, Kore University of Enna, Enna, Italy;
[4]Department of Neurological Surgery, University of California, Davis, Sacramento, CA, U.S.A.;
[5]Neurosurgical Unit, Department of Biomedicine, Neurosciences and Advanced Diagnostics (BiND), University of Palermo, Palermo, Italy;
[6]Radiology Unit, Giovanni Paolo II Hospital, Ragusa, Italy;
[7]Neurosurgery Unit, Department of Head and Neck Surgery, Garibaldi Hospital, Catania, Italy

## Abstract

*Background/Aim:* This study compared dosimetric differences in target coverage and organs-at-risk (OARs) sparing among coplanar (co-VMAT), non-coplanar (nonco-VMAT), and mixed-arc (mxd-VMAT) volumetric modulated arc therapy (VMAT) for stereotactic radiation treatment of head and face skin cancers (HFSC).

*Patients and Methods:* Five patients with HFSC, presenting with tumors located in critical areas near OARs were selected to represent distinct clinical scenarios. At least three competing VMAT plans per case (up to five for extensive tumors) were generated. The planning target volume (PTV) was obtained by applying a 1 mm isotropic expansion to the clinical target volume (CTV), except for portions extending beyond the body contour. Dosimetric parameters, including PTV indices [Dmax, D2%, D98%, V95%, conformity index (CI), and homogeneity index (HI)], dose to surrounding healthy tissues, beam-on time (BOT), and monitor units (MU) were evaluated and compared under identical optimization conditions.

*Results:* Nonco-VMAT improved CI, HI, and OAR sparing for the first (left temporal-zygomatic) and third (nasal pyramid) patients. For the second patient (right frontal and zygomatic targets), mxd-VMAT was optimal for the frontal target, while nonco-VMAT was superior for the zygomatic target. Co-VMAT provided the highest plan quality for the fourth (occipital) patient, though mxd-VMAT slightly reduced OAR doses. For the fifth patient (scalp and vertex), co-VMAT achieved the best balance between target coverage and OAR sparing.

*continued*

Gianluca Ferini, MD, REM Radioterapia srl, Via Penninazzo 11, 95029, Viagrande (CT), Italy. Tel: +39 0957899569, e-mail: gianluca.ferini@grupposamed.com

Received February 23, 2025 | Revised March 19, 2025 | Accepted March 24, 2025

*Conclusion:* This study highlights the potential benefits of non-coplanar arcs in HFSC treatment. VMAT arc arrangement should be tailored to tumor location, as the inclusion of non-coplanar arcs can enhance plan quality for both target coverage and OAR protection in specific cases. However, non-coplanar techniques may prolong treatment duration due to couch rotations and increased MU, potentially reducing patient tolerability.

**Keywords:** Head and face, skin, cancer, VMAT, coplanar, non-coplanar, mixed-arc, radiotherapy.

## Introduction

Radiotherapy (RT) for head and face skin cancers (HFSC) poses significant challenges due to the proximity of highly radiosensitive organs at risk (OARs), such as the brain, lenses, and lacrimal glands (1-4). For instance, in the treatment of scalp tumors, the penetration depth of high-energy (MeV) photons complicates the effective sparing of underlying brain tissue. As a result, low-energy (kV) photons and electron beams are often considered preferable alternatives (5, 6). While kV photons have become increasingly uncommon due to the progressive replacement of roentgen therapy equipment with modern linear accelerators (LINACs), LINAC-based electron beam radiotherapy (EBRT) remains a widely used and valid therapeutic option for HFSC (7).

EBRT is characterized by a steeper dose fall-off compared to MeV photons, reducing energy deposition beyond the target volume and thereby sparing adjacent healthy tissues. Typically, EBRT is delivered using an en face field, manually collimated with lead cutouts of various sizes and shapes to conform to the tumor geometry. The choice of electron energy and prescription isodose is guided primarily by tumor thickness (8). However, this approach is inherently imprecise, as it does not allow for rigorous control of the dose delivered to neighboring OARs (9). Furthermore, anatomical irregularities, such as those found in large scalp tumors or periorbital and nasal lesions, can cause significant dose perturbations within the target, leading to hot and cold spots that may increase toxicity or compromise local tumor control (10). These limitations arise because EBRT is most effective on flat surfaces, which are rarely encountered in the head and face region.

To mitigate these drawbacks, advanced electron dose calculation algorithms have been integrated into certain treatment planning systems (TPS), leading to the development of modulated electron radiotherapy (MERT) (11). However, these newer EBRT techniques remain largely unavailable, and their implementation is hindered by a lack of familiarity among radiation physicists (12). Consequently, photon-based RT, calculated *via* TPS, is often preferred over EBRT.

Compared to electrons, photon beams exhibit a more gradual dose fall-off in healthy tissues for the same prescription dose, thereby increasing the risk of radiation-induced toxicity. One strategy to minimize unnecessary OAR exposure is to optimize beam path distribution across multiple angles, either within the same plane or across different planes. This optimization is achievable through volumetric modulated arc therapy (VMAT) and non-isocentric robotic systems, such as CyberKnife (13, 14).

VMAT can be delivered using either coplanar arcs (with the treatment couch fixed at 0°) or non-coplanar arcs (with non-zero couch angles). The latter configuration has been shown to enhance OAR sparing in various tumor sites without compromising target coverage (15-17). However, the safe delivery of non-coplanar arcs requires precise setup verification, as even minimal positional errors introduced by couch rotation can impact dose distribution. Dedicated image-guidance systems, such as ExacTrac, facilitate accurate patient positioning and correction of setup deviations (18).

In this study, we evaluated the dosimetric differences in OAR and planning target volume (PTV) coverage among coplanar, non-coplanar, and mixed VMAT plans in five

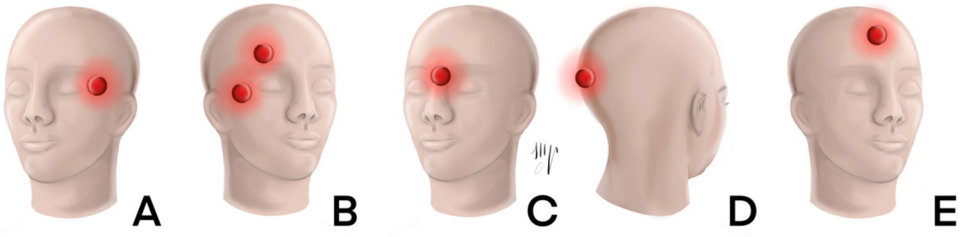


Figure 1. *Tumor sites for the five illustrative cases. Panels A, B, C, D, and E represent the first, second, third, fourth, and fifth scenarios, respectively. The red pointer marks the affected areas; however, its dimensions are not to scale with the tumor's size and shape.*

representative HFSC cases, using stereotactic dose delivery under ExacTrac guidance.

## Patients and Methods

*Compliance with ethical standards.* This article does not involve any studies conducted by the authors on animals. All procedures carried out in studies involving human participants adhered to the ethical standards set by the institutional and/or national research committee, following the 1964 Helsinki Declaration and its subsequent amendments or equivalent ethical standards. Informed consent was obtained from the participants included in the study.

*Illustrative teaching scenarios.* Five cases of skin cancer located in critical head and face areas, with tumors closely abutting the brain or eyes, were selected to evaluate the dosimetric differences between coplanar, non-coplanar, and mixed treatment plans (Figure 1). All patients were immobilized in the supine position using thermoplastic masks and underwent computed tomography (CT) simulation with a slice thickness of 1.25 mm. A 5-mm thick bolus was applied on a case-by-case basis.

Following CT acquisition, images were imported into the Eclipse treatment planning system (TPS) (version 13.7, Varian Medical Systems, Palo Alto, CA, USA). The following volumes of interest were contoured: the clinical target volume (CTV), encompassing the macroscopic disease (gross tumor volume, GTV) and surrounding tissues at risk for subclinical tumor infiltration; the planning target volume (PTV), obtained by a 1 mm isotropic expansion of the CTV (excluding extensions beyond the body surface) to account for setup uncertainties; and the organs at risk (OARs), including the brain, eyes, and lenses. In cases of periorbital tumors, the lacrimal glands were also contoured.

Dose prescriptions were assigned based on tumor histology, with lower doses for basal cell carcinoma (BCC) and Merkel cell carcinoma (MCC) compared to cutaneous squamous cell carcinoma (CSCC).

*Treatment planning.* For each patient, three VMAT techniques were compared: Coplanar VMAT (co-VMAT) using only coplanar arcs; Non-coplanar VMAT (nonco-VMAT) using only non-coplanar arcs; Mixed VMAT (mxd-VMAT) combining both coplanar and non-coplanar arcs, incorporating the same couch angles as in nonco-VMAT while also including arcs at 0˚ couch angle, as in co-VMAT.

Treatment plans were created for a TrueBeam Novalis STx linear accelerator equipped with a high-definition multileaf collimator and 6 MeV flattening filter-free photon beams. Non-coplanar arcs were planned with five couch rotations: 30˚, 60˚, 270˚, 300˚, and 330˚. These angles were simultaneously considered in all cases, except for the most extended PTVs (>100 cc) on the head surface, where the effect of reducing the number of non-coplanar arcs on the dose distribution was also evaluated.

*Dosimetric evaluation.* The planning objective for the PTV was to achieve at least 98% coverage of the target volume

with 95% of the prescription dose (D98% >95%), following International Commission on Radiation Units and Measurements (ICRU) 83 recommendations (19). In specific cases, D95% >95% was considered sufficient, while for complex target geometries, D90% >90% was deemed an acceptable goal.

The following dosimetric parameters were analyzed: 1) Target coverage and dose homogeneity: i) D98% (near-minimum dose), D2% (near-maximum dose), and D50% (median dose) were used to calculate the homogeneity index (HI) using the formula: HI=(D2%−D98%)/D50%, where values approaching 0 indicate better homogeneity. ii) The Paddick conformity index (CI) was used to assess the conformity of the 95% isodose to the PTV (20), with values approaching 1 indicating superior conformity. iii) The maximum dose (Dmax) was intended to be limited to 110% of the prescribed dose. 2) OAR dose constraints: i) The Dmax and mean dose (Dmean) were recorded for all OARs. ii) For the brain, the volumes receiving 70% (V70%) and 50% (V50%) of the prescribed dose were reported. iii) For cases where significant brain irradiation was expected (*e.g*., scalp tumors), additional avoidance structures were delineated to minimize brain dose.

All dose distributions were analyzed using dose-volume histograms. Intra-patient comparisons of the VMAT plans were conducted using identical optimization parameters for each case, as detailed in Supplementary Materials 1 and 2.

*Image-guided radiation therapy (IGRT) and delivery time comparison*. Given the high doses per fraction, an accurate strategy is essential to assess the feasibility of non-coplanar arcs. At our center, setup verification relies on cone-beam CT for bone and soft tissue matching when the treatment couch is positioned at 0°, and on high-resolution kV images from ExacTrac 6.2.3 (Brainlab, Munich, Germany) for precise skull bone alignment at non-zero couch angles. A robotic treatment couch with six degrees of freedom allows for the correction of both translational and rotational setup errors.

Additionally, co-VMAT, nonco-VMAT, and mxd-VMAT plans were compared in terms of total monitor units (MUs) and beam-on time (BOT).

## Results

*First scenario: left temporal-zygomatic site.* An 83-year-old male with a history of actinic keratosis of the head and face underwent excisional biopsy of a lesion in the left temporal region. Postoperative pathology revealed G3 squamous cell carcinoma with positive margins, leading to a referral to our radiotherapy department. Co-VMAT, nonco-VMAT, and mxd-VMAT plans were subsequently generated and compared.

The prescribed dose was 30 Gy in five fractions, to be delivered twice weekly, with each plan normalized to ensure 98% target volume coverage. A 5-mm thick bolus was included in all plans to improve target coverage. Dose distribution and beam arrangements are shown in Figure 2, while Supplementary Material 3 provides details on couch, collimator, and gantry angles. Dose-volume parameters for the PTV and OARs, as well as MU and BOT values, are also reported.

Overall, the nonco-VMAT plan demonstrated superior dosimetric performance, achieving better conformity index (CI) and homogeneity index (HI), along with a lower hotspot compared to the other two techniques. Additionally, it resulted in improved OAR sparing. No differences in MU or BOT were observed among the three modalities.

*Second scenario: Right temporal-zygomatic and frontal sites.* A 90-year-old female was referred to our department following multiple recurrences of G3 squamous cell carcinomas of the head and face, previously managed with surgery. Due to the extent of the latest recurrence in the right temporal-zygomatic and frontal regions, further resection was deemed unfeasible, and radiotherapy consultation was indicated. Both lesions were planned to receive 35 Gy in 5 fractions.

For each target, three VMAT plans were generated. The collimator, gantry, and couch angle configurations used for plan generation are detailed in Supplementary Materials 4 and 5. All VMAT plans were normalized to ensure 98% of the PTV received at least 95% of the prescribed dose (Figure 3, Figure 4). No bolus was applied.

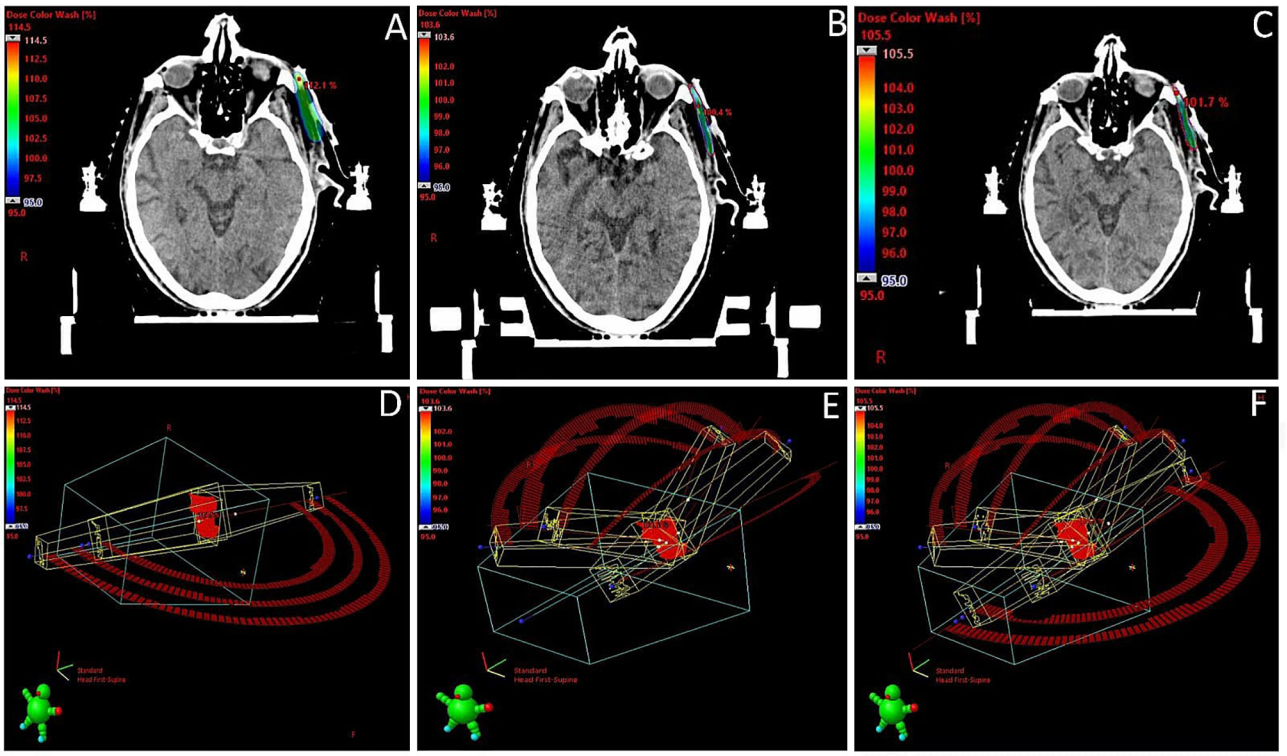


Figure 2. *Dose distribution to the left temporal-zygomatic target and beam trajectories. Panels A, B, and C (top) show the 95% isodose distribution for the co-VMAT, nonco-VMAT, and mxd-VMAT plans, respectively. Panels D, E, and F (bottom) display the corresponding beam arrangements for each plan.*

For the frontal target, none of the techniques achieved a maximum point dose below 110% of the prescription, though the mxd-VMAT plan was closest to this threshold (114%). The nonco-VMAT plan exhibited the highest Dmax (119.3%). Conversely, for the temporal-zygomatic target, both the nonco-VMAT (107.2%) and mxd-VMAT (108.7%) plans maintained acceptable Dmax values.

In terms of plan quality, the mxd-VMAT approach yielded a slightly superior HI for both tumor sites while maintaining CI comparable to the respective co-VMAT and nonco-VMAT plans. Regarding OAR sparing, the co-VMAT plan resulted in significantly higher doses to OARs for the right temporal-zygomatic target, whereas differences were negligible for the frontal target, except for the brain Dmax, which was lower in the mxd-VMAT plan. Plan sum evaluations confirmed no significant reciprocal dosimetric influence between targets. BOT was slightly longer with the nonco-VMAT technique for both sites.

Supplementary Materials 4 and 5 provide a detailed comparison of PTV indices, OAR dose parameters, MU, and BOT for the frontal and temporal-zygomatic targets, respectively. The OAR dose parameters derived from the plan sum analysis are reported at the end of Supplementary Material 5.

*Third scenario: Nasal pyramid site.* An 80-year-old patient with a history of MCC of the parotid gland, previously treated with surgery, chemotherapy, and radiotherapy, was referred to our center owing to disease progression at multiple sites. Among these, a bulky lesion (6.91×3.20 cm) had developed at the root of the nose and was refractory to avelumab. A dose of 25 Gy in five daily fractions was prescribed for this target and planned using the three VMAT arrangements. Dose normalization was set to ensure that the 95% isodose of the prescribed dose covered at least 95% of the target volume. To optimize target coverage, a 5-mm-thick bolus was applied.

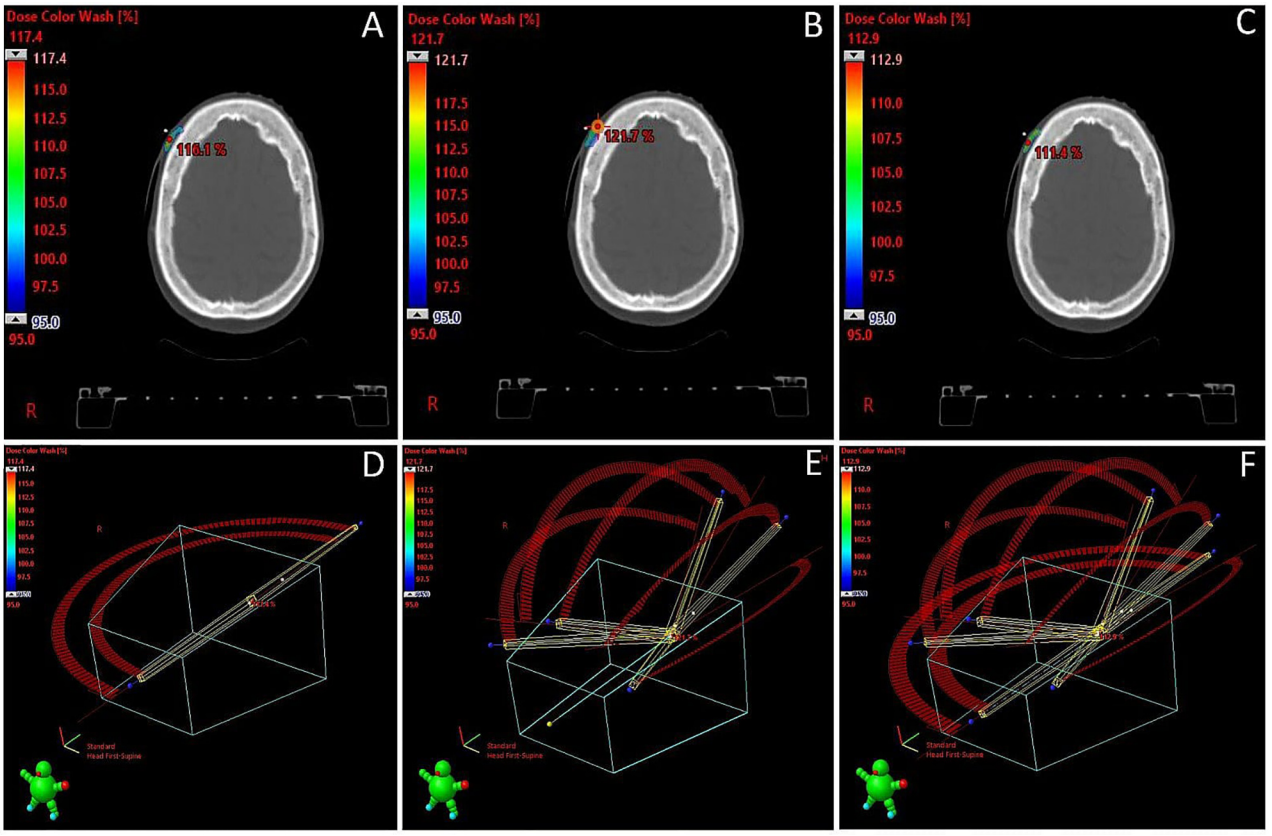


Figure 3. *Dose distribution to the frontal target and beam trajectories. Panels A, B, and C (top) show the 95% isodose distribution for the co-VMAT, nonco-VMAT, and mxd-VMAT plans, respectively. Panels D, E, and F (bottom) display the corresponding beam arrangements for each plan.*

Figure 5 illustrates the 95% dose coverage and arc arrangement for each plan, while Supplementary Material 6 provides details on the couch, collimator, and gantry settings. In terms of PTV indices, the nonco-VMAT plan demonstrated significant superiority. This advantage was also evident in OAR sparing, without a notable increase in BOT (Supplementary Material 6).

*Fourth scenario: Occipital site.* A 77-year-old male with a history of actinic keratosis was referred to our radiotherapy department following an excisional biopsy of a scalp lesion, which revealed G2 squamous cell carcinoma infiltrating the dermis and resection margins. Consequently, a total dose of 35 Gy in five fractions was planned using a 5-mm bolus and the three competing VMAT approaches, which were then compared. Dose normalization was set to ensure that 95% of the prescribed dose covered 98% of the target volume (Figure 6). The couch, collimator, and gantry angles are detailed in Supplementary Material 7.

Regarding PTV parameters, the co-VMAT plan outperformed the nonco-VMAT and mxd-VMAT plans when using five non-coplanar arcs. The suboptimal results observed with five non-coplanar arcs (nonco-VMAT 5x), even when combined with two coplanar ones (mxd-VMAT 7x), prompted an evaluation of alternative arc configurations. By reducing the number of non-coplanar arcs, we identified that adding only the two least divergent non-coplanar arcs (30° and 330°) to the coplanar ones provided a certain degree of OAR sparing, particularly for

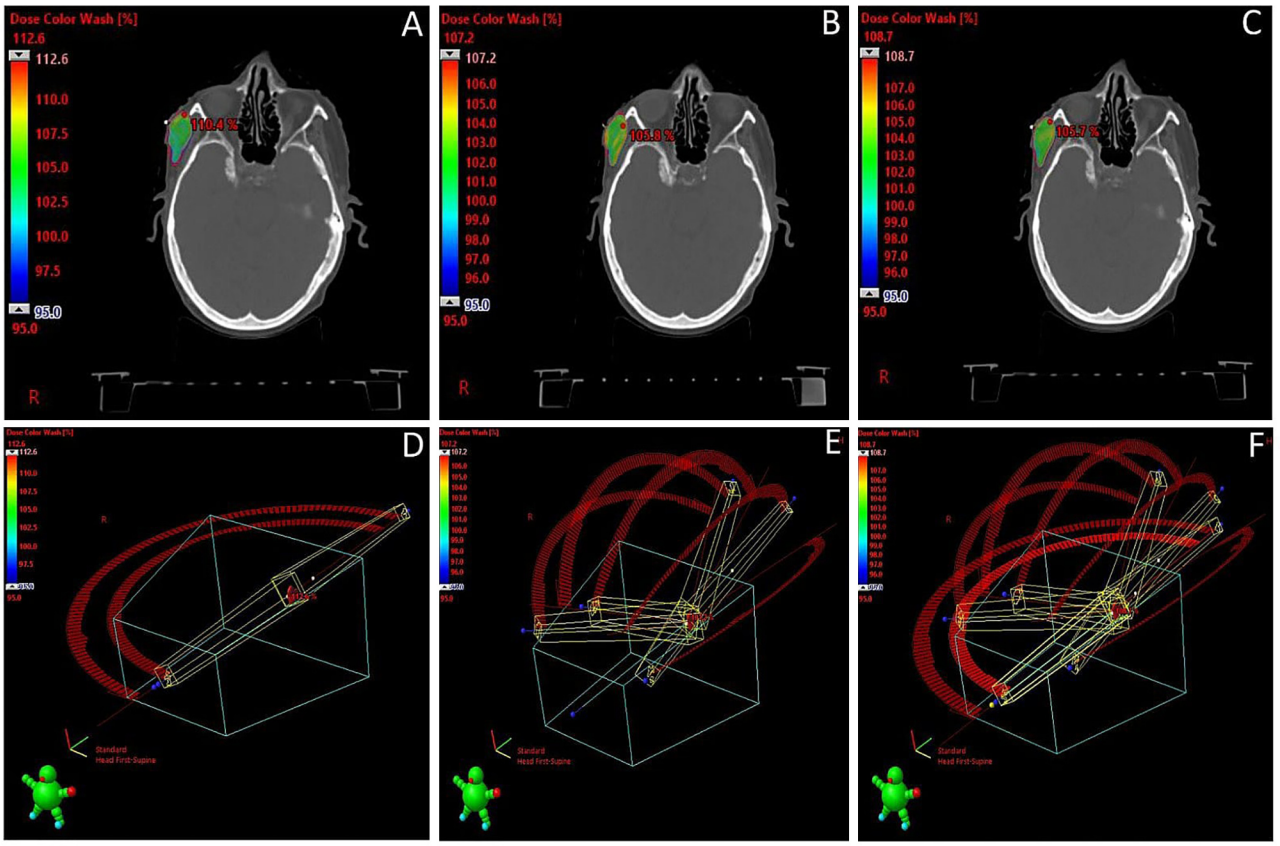


Figure 4. *Dose distribution to the right temporal-zygomatic target and beam trajectories. Panels A, B, and C (top) show the 95% isodose distribution for the co-VMAT, nonco-VMAT, and mxd-VMAT plans, respectively. Panels D, E, and F (bottom) display the corresponding beam arrangements for each plan.*

brain Dmean, as well as eye and lens dose parameters, without compromising PTV coverage. As a result, the mxd-VMAT 4x plan emerged as the most balanced solution. However, this plan had the second-longest BOT.

*Fifth scenario: Scalp and vertex targets*. An 89-year-old male in fair general condition was referred to our department for an extensive squamous cell carcinoma of the scalp. The prescribed dose was 32 Gy in four fractions, delivered twice weekly to an extended CTV, followed by an 8 Gy boost to a smaller area (GTV). The three competing VMAT techniques were tested using a 5-mm bolus for each target. Given the complexity of the extended scalp target, dose normalization was set to ensure that 90% of the prescribed dose covered 95% of the target volume (Figure 7 and Figure 8). For the boost plan, encompassing only the GTV, normalization ensured that 95% of the prescribed dose covered 95% of the target volume. The couch, collimator, and gantry angles are detailed in Supplementary Materials 8 and 9.

As in the previous case, solutions with fewer non-coplanar arcs were explored. The co-VMAT plan emerged as the best approach for both the initial and boost treatments. In the extended CTV plan, the only configuration that approached the performance of co-VMAT was the mxd-VMAT 4x plan, which reduced brain tissue exposure to medium doses (V50%, 260.38 cc *vs.* 342.37 cc). However, the mxd-VMAT 4x plan failed to meet all remaining dosimetric objectives, as did the other plans, which performed even worse. Similar trends were

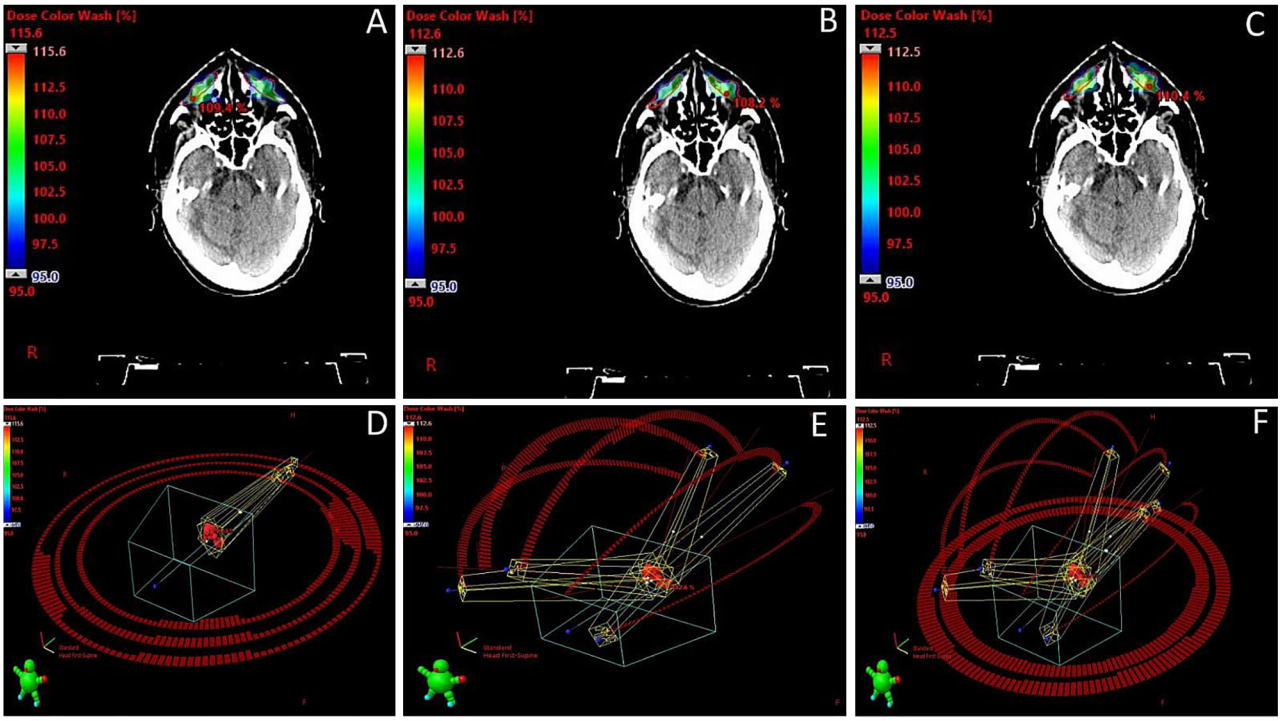


Figure 5. *Dose distribution to the nasal pyramid target and beam trajectories. Panels A, B, and C (top) show the 95% isodose distribution for the co-VMAT, nonco-VMAT, and mxd-VMAT plans, respectively. Panels D, E, and F (bottom) display the corresponding beam arrangements for each plan.*

observed in the boost plan. Notably, the co-VMAT plans had the longest BOT among all techniques.

Supplementary Materials 8 and 9 summarize the dosimetric characteristics of the five plans, including PTV indices, OAR sparing, MU, and BOT for both the extended scalp target and the boost plan. The OAR dose parameters from the plan sums are provided at the end of Supplementary Material 9.

## Discussion

To our knowledge, this is the first study specifically dedicated to assessing the usefulness of non-coplanar VMAT in treating cutaneous malignancies of the head and face. Existing reports on such arc arrangements primarily concern mucosal head and neck cancers, which, being located deeper, are more suitable for high-energy photon-based RT (16). Historically, kilovoltage roentgen therapy and electron beam RT have been preferred over megavoltage (MeV) photon-based RT due to their superior percentage depth dose curves, which spare underlying healthy tissues while achieving increased superficial dose deposition (21). However, as discussed earlier, both techniques have significant limitations (6). While MeV photon-based RT offers more precise dose distribution and greater adaptability for treating targets with curved shapes or variable thickness, it also results in higher OAR exposure to radiation (22). Increasing photon beam paths could improve both target coverage and OAR sparing. To test this hypothesis, we simulated VMAT plans with and without non-coplanar arcs in five distinct clinical scenarios.

Curative RT doses can be delivered through conventional fractionation (1.8-2 Gy/day) or ultra-hypofractionated schedules (≥5 Gy/fraction) (8). Skin cancers are more prevalent in elderly patients, whose comorbidities may limit compliance with long-course RT

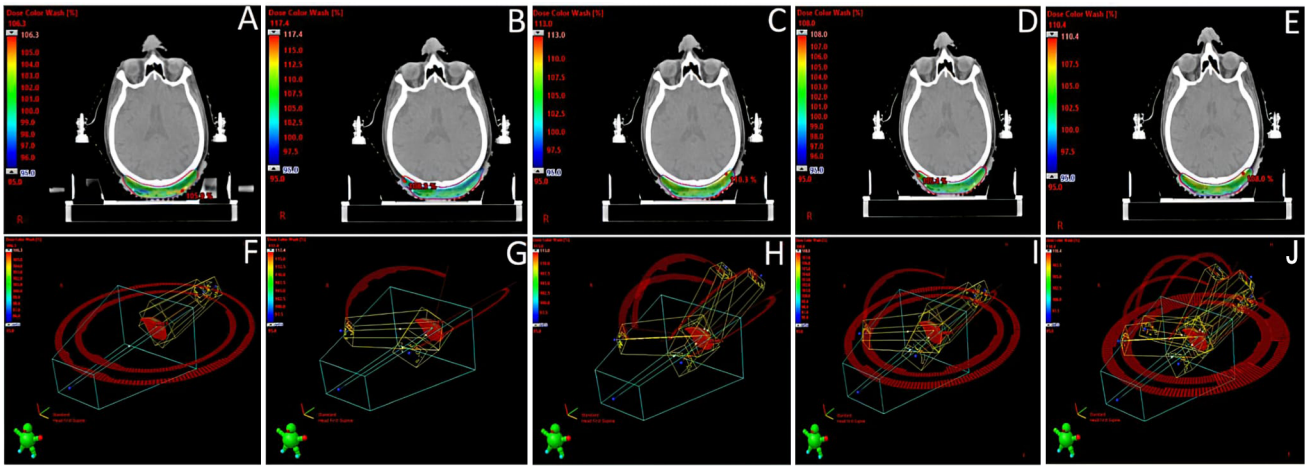


Figure 6. *Dose distribution to the occipital target and beam trajectories. Panels A, B, C, D, and E (top) show the 95% isodose distribution for the co-VMAT, nonco-VMAT 2x, nonco-VMAT 5x, mxd-VMAT 4x, and mxd-VMAT 7x plans, respectively. Panels F, G, H, I, and J (bottom) display the corresponding beam arrangements for each plan.*

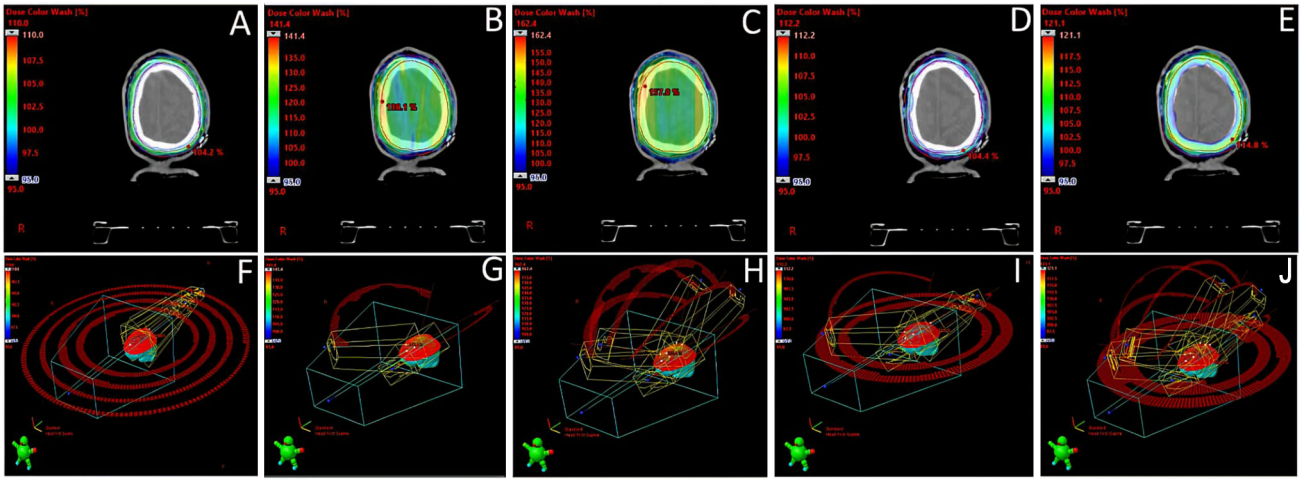


Figure 7. *Dose distribution to the extended scalp target and beam trajectories. Panels A, B, C, D, and E (top) show the 95% isodose distribution for the co-VMAT, nonco-VMAT 2x, nonco-VMAT 5x, mxd-VMAT 4x, and mxd-VMAT 7x plans, respectively. Panels F, G, H, I, and J (bottom) display the corresponding beam arrangements for each plan.*

(23). Hypofractionation offers the advantage of reducing daily clinic visits while improving local control, as supported by recent evidence favoring dose escalation with stereotactic RT protocols (24). However, high-dose fractions also increase the risk of radiation-induced toxicity in peri-target OARs. This is particularly concerning when treating facial and scalp lesions, where OAR exposure must be carefully evaluated (25). The brain, in particular, is highly radiosensitive, especially in elderly patients, where radiation-induced cognitive impairment may be mistaken for age-related decline. Thus, its exposure should be minimized, as no radiation dose is entirely without risk (1). Conversely, the eyes, lenses, and lacrimal glands are generally well spared in stereotactic RT for HFSCs, even when located near the orbit (26). Given the high propensity for recurrence of these tumors and

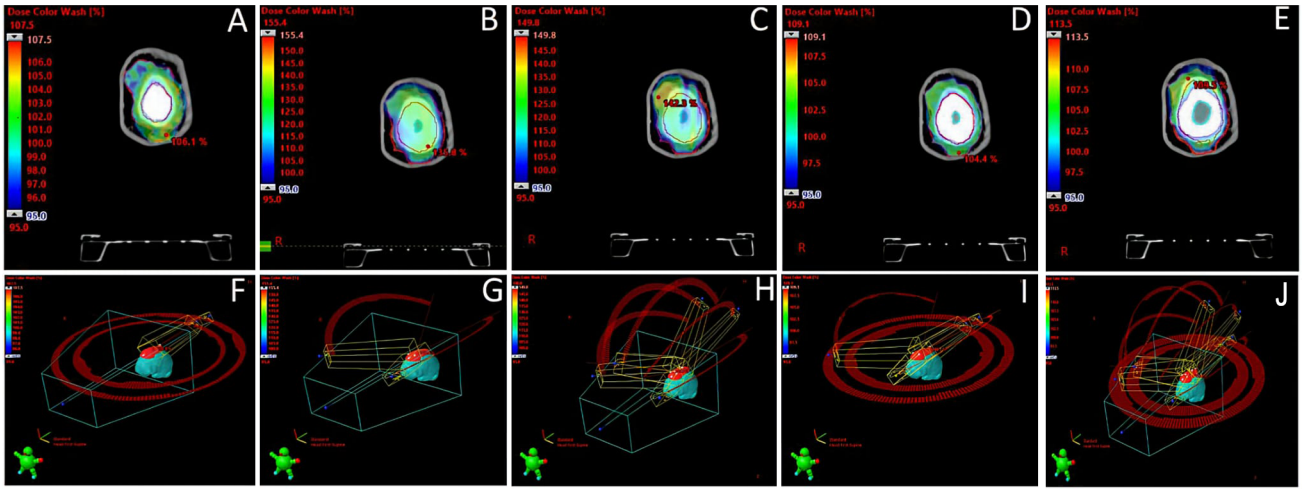


Figure 8. *Dose distribution to the vertex target and beam trajectories. Panels A, B, C, D, and E (top) show the 95% isodose distribution for the co-VMAT, nonco-VMAT 2x, nonco-VMAT 5x, mxd-VMAT 4x, and mxd-VMAT 7x plans, respectively. Panels F, G, H, I, and J (bottom) display the corresponding beam arrangements for each plan.*

the potential need for re-irradiation, OAR dose constraints should adhere to the ALARA (As Low As Reasonably Achievable) principle to minimize cumulative toxicity (27). These considerations underscore the importance of advanced RT techniques that enhance target coverage while minimizing OAR exposure.

Our study demonstrated that non-coplanar VMAT arcs offer advantages in certain anatomical sites. In Case 1, the nonco-VMAT plan provided the best balance between dose homogeneity, conformity, and OAR sparing due to the tangential photon beam entrance to the temporal target, particularly when the couch angle was 270°. This configuration maximized the tangential effect, further enhanced by a bolus compensating for the build-up region underdosing. Consequently, dose deposition beyond the inner layer of the skin target was reduced, improving conformity index (CI) and sparing underlying tissues compared to co-VMAT and mxd-VMAT plans. Rotational RT techniques inherently mitigate the skin-sparing build-up effect of high-energy photons by gradually making the radiation beam oblique to the skin surface (28). Accordingly, Cases 1 and 2, which had mirrored temporal-zygomatic targets (left in Case 1, right in Case 2), achieved optimal dosimetric results with non-coplanar arcs alone, even in the absence of bolus in Case 2. In contrast, for the frontal target in Case 2, the best-performing plan was the mxd-VMAT approach.

In Case 3, involving a bulky nasal root tumor partially obstructing vision, the nonco-VMAT plan significantly reduced dose exposure to all OARs, particularly the brain and lenses, while maintaining adequate target coverage and homogeneity.

In Case 4, the occipital target benefited most from the mxd-VMAT 4x plan, which achieved comparable PTV dosimetric parameters while slightly improving brain sparing compared to nonco-VMAT and co-VMAT plans.

Lastly, for the scalp target in Case 5, the co-VMAT plan outperformed all others for both the large CTV and smaller GTV boost. The concave shape of the scalp target encompassed a substantial portion of the brain, leading to a significantly higher mean brain dose than in the other cases. The mxd-VMAT approach further increased this dose due to oblique beam exits traversing the brain caudal to the scalp target's inferior border. However, adding two minimally angled non-coplanar arcs (30° and 330°) to coplanar ones helped reduce medium-dose brain

exposure (V50%) by increasing beam path dispersion. Notably, our TPS was unable to generate a satisfactory and deliverable nonco-VMAT plan for this case, making it the least favorable option.

By analyzing these five clinical scenarios, this study highlights the potential benefits of non-coplanar VMAT in HFSC treatment, identifying tumor sites where it is advantageous and where it may be counterproductive. However, safe implementation requires specific considerations. First, the critical anatomical location of HFSC necessitates meticulous setup verification to prevent both target miss and unintended OAR overexposure. We routinely employ the ExacTrac system, which reliably fulfils this task (29). Facilities lacking similar verification systems should be cautious in adopting non-coplanar arcs due to concerns about intrafraction motion during couch rotation. Second, the arc arrangements tested here do not necessarily represent the optimal configurations. Advanced path-finding algorithms could refine beam arrangements (30), but their discussion lies beyond this article's scope. Furthermore, the presence of surgical meshes, particularly titanium ones used for scalp cranioplasty, can cause dose perturbations such as backscattering to the skin flap (31). Finally, nonco-VMAT treatments generally require longer delivery times due to couch rotations and potentially increased MU requirements for adequate target coverage, which may affect patient compliance and comfort.

Given the variability in HFSC size, shape, and proximity to critical structures, no universal arc configuration can be recommended. Each case demands individualized beam arrangement optimization. This study offers insight into the potential dosimetric advantages of different VMAT strategies, encouraging practitioners to explore alternative solutions while carefully considering collision risks between the gantry and couch. The couch angles tested here were adapted from our standard intracranial stereotactic RT template (32), chosen for their uniform 30˚ spacing, which optimizes beam trajectory expansion without excessively prolonging treatment time.

## Conclusion

This study is the first to demonstrate the potential advantages of incorporating non-coplanar arcs in the treatment of head and face skin cancers using commonly available LINACs and TPS platforms. While these five cases do not encompass all possible HFSC presentations, they offer practical guidance for treatment planning and challenge dosimetrists to refine VMAT strategies for improved therapeutic outcomes. Our findings underscore the need to individualize VMAT arc arrangements based on tumor location, as the addition of non-coplanar arcs may improve plan quality by enhancing target coverage and sparing organs at risk in selected cases. However, their implementation requires meticulous verification to avoid both missing the target and delivering excessive radiation doses to OARs. Moreover, the increased treatment duration associated with couch rotations and potentially higher monitor unit requirements may affect patient compliance and comfort compared to fully coplanar approaches. Further studies are warranted to validate these findings and refine arc selection strategies for clinical practice.

## Supplementary Material

Available at: https://www.dropbox.com/scl/fi/746v86kvqqdabhf1y2nua/Suppl.-materials-VMAT-def.pdf?rlkey=086p4hqeiaiv9ff3g28ndkp1z&st=huq7mv04&dl=0

## Conflicts of Interest

The Authors have no conflicts of interest to declare in relation to this study.

## Authors' Contributions

VZ collected patient data and contributed to drafting the first version; DLF performed dosimetric analysis; GEU, SL, PP, MN, AB, and GS provided critical analysis; GF conceptualized the project, contributed to drafting the

first version, and revised the final manuscript. All Authors approved the final manuscript.

## Funding

This manuscript did not receive any funds.

## References

1 Gan C, Li W, Xu J, Pang L, Tang L, Yu S, Li A, Ge H, Huang R, Cheng H: Advances in the study of the molecular biological mechanisms of radiation-induced brain injury. Am J Cancer Res 13(8): 3275-3299, 2023.
2 Nanda T, Wu CC, Campbell AA, Bathras RM, Jani A, Kazim M, Wang TJC: Risk of dry eye syndrome in patients treated with whole-brain radiotherapy. Med Dosim 42(4): 357-362, 2017. DOI: 10.1016/j.meddos.2017.07.007
3 Arefpour AM, Bahrami M, Haghparast A, Khoshgard K, Aryaei Tabar H, Farshchian N: Evaluating dose-response of cataract induction in radiotherapy of head and neck cancers patients. J Biomed Phys Eng 11(1): 9-16, 2021. DOI: 10.31661/jbpe.v0i0.834
4 Orton A, Gordon J, Vigh T, Tonkin A, Cannon G: Differences in parotid dosimetry and expected normal tissue complication probabilities in whole brain radiation plans covering C1 versus C2. Cureus 9(5): e1217, 2017. DOI: 10.7759/cureus.1217
5 Bodner WR, Hilaris BS, Alagheband M, Safai B, Mastoras CA, Saraf S: Use of low-energy X-rays in the treatment of superficial nonmelanomatous skin cancers. Cancer Invest 21(3): 355-362, 2003. DOI: 10.1081/cnv-120018226
6 Wilmas KM, Garner WB, Ballo MT, McGovern SL, MacFarlane DF: The role of radiation therapy in the management of cutaneous malignancies. Part I: Diagnostic modalities and applications. J Am Acad Dermatol 85(3): 539-548, 2021. DOI: 10.1016/j.jaad.2021.05.058
7 Levendag PC, Vermey J, Senan S: The history of radiotherapy in the Netherlands. Int J Radiat Oncol Biol Phys 35(3): 615-622, 1996. DOI: 10.1016/s0360-3016(96)80027-7
8 Ferini G, Molino L, Bottalico L, De Lucia P, Garofalo F: A small case series about safety and effectiveness of a hypofractionated electron beam radiotherapy schedule in five fractions for facial non melanoma skin cancer among frail and elderly patients. Rep Pract Oncol Radiother 26(1): 66-72, 2021. DOI: 10.5603/RPOR.a2021.0013
9 Ali I, Kendall E, Alsbou N, Ahmad S: Quantitative evaluation of dosimetric uncertainties associated with small electron fields. J Med Imaging Radiat Sci 53(2): 273-282, 2022. DOI: 10.1016/j.jmir.2022.02.007
10 Maemoto H, Iraha S, Arashiro K, Ishigami K, Ganaha F, Murayama S: Risk factors of recurrence after postoperative electron beam radiation therapy for keloid: Comparison of long-term local control rate. Rep Pract Oncol Radiother 25(4): 606-611, 2020. DOI: 10.1016/j.rpor.2020.05.001
11 Surucu M, Klein EE, Mamalui-Hunter M, Mansur DB, Low DA: Planning tools for modulated electron radiotherapy. Med Phys 37(5): 2215-2224, 2010. DOI: 10.1118/1.3395573
12 Henzen D, Manser P, Frei D, Volken W, Neuenschwander H, Born EJ, Lössl K, Aebersold DM, Stampanoni MFM, Fix MK: Forward treatment planning for modulated electron radiotherapy (MERT) employing Monte Carlo methods. Med Phys 41(3): 031712, 2014. DOI: 10.1118/1.4866227
13 Nicolini G, Abraham S, Fogliata A, Jordaan A, Clivio A, Vanetti E, Cozzi L: Critical appraisal of volumetric-modulated arc therapy compared with electrons for the radiotherapy of cutaneous Kaposi's sarcoma of lower extremities with bone sparing. Br J Radiol 86(1023): 20120543, 2013. DOI: 10.1259/bjr.20120543
14 Pontoriero A, Iatì G, Pergolizzi S: A case report of a patient with squamous cell carcinoma of the face irradiated using a stereotactic technique. Radiat Oncol J 33(3): 261-264, 2015. DOI: 10.3857/roj.2015.33.3.261
15 Sharfo AWM, Rossi L, Dirkx MLP, Breedveld S, Aluwini S, Heijmen BJM: Complementing prostate SBRT VMAT with a two-beam non-coplanar IMRT class solution to enhance rectum and bladder sparing with minimum increase in treatment time. Front Oncol 11: 620978, 2021. DOI: 10.3389/fonc.2021.620978
16 Gayen S, Kombathula SH, Manna S, Varshney S, Pareek P: Dosimetric comparison of coplanar and non-coplanar volumetric-modulated arc therapy in head and neck cancer treated with radiotherapy. Radiat Oncol J 38(2): 138-147, 2020. DOI: 10.3857/roj.2020.00143
17 Cheung EYW, Lee KHY, Lau WTL, Lau APY, Wat PY: Non-coplanar VMAT plans for postoperative primary brain tumour to reduce dose to hippocampus, temporal lobe and cochlea: a planning study. BJR Open 3(1): 20210009, 2021. DOI: 10.1259/bjro.20210009
18 Lai JL, Liu SP, Jiang XX, Liu J, Li A, Li B, Li XK, Ye XJ, Lei KJ, Zhou L: Can optical surface imaging replace non-coplanar cone-beam computed tomography for non-coplanar set-up verification in single-isocentre non-coplanar stereotactic radiosurgery and hypofractionated stereotactic radiotherapy for single and multiple brain metastases? Clin Oncol (R Coll Radiol) 35(12): e657-e665, 2023. DOI: 10.1016/j.clon.2023.09.007
19 Grégoire V, Mackie TR: State of the art on dose prescription, reporting and recording in Intensity-Modulated Radiation Therapy (ICRU report No. 83). Cancer Radiother 15(6-7): 555-559, 2011. DOI: 10.1016/j.canrad.2011.04.003
20 Feuvret L, Noël G, Mazeron JJ, Bey P: Conformity index: A review. Int J Radiat Oncol Biol Phys 64(2): 333-342, 2006. DOI: 10.1016/j.ijrobp.2005.09.028

21 Amdur RJ, Kalbaugh KJ, Ewald LM, Parsons JT, Mendenhall WM, Bova FJ, Million RR: Radiation therapy for skin cancer near the eye: Kilovoltage x-rays *versus* electrons. Int J Radiat Oncol Biol Phys 23(4): 769-779, 1992. DOI: 10.1016/0360-3016(92)90650-7
22 Alexander A, Soisson E, Hijal T, Sarfehnia A, Seuntjens J: Comparison of modulated electron radiotherapy to conventional electron boost irradiation and volumetric modulated photon arc therapy for treatment of tumour bed boost in breast cancer. Radiother Oncol 100(2): 253-258, 2011. DOI: 10.1016/j.radonc.2011.05.081
23 Osong B, Bermejo I, Lee KC, Lee SH, Dekker A, van Soest J: Prediction of radiotherapy compliance in elderly cancer patients using an internally validated decision tree. Cancers (Basel) 14(24): 6116, 2022. DOI: 10.3390/cancers14246116
24 Voruganti IS, Poon I, Husain ZA, Bayley A, Barnes EA, Zhang L, Chin L, Erler D, Higgins K, Enepekides D, Eskander A, Karam I: Stereotactic body radiotherapy for head and neck skin cancer. Radiother Oncol 165: 1-7, 2021. DOI: 10.1016/j.radonc.2021.10.004
25 Ferini G, Fichera C, Boncoraglio A, Umana GE, Forte S: De Felice scheme: No risk at all of brain radionecrosis? Head Neck 46(10): 2661-2663, 2024. DOI: 10.1002/hed.27853
26 Pontoriero A, Iatì G, Conti A, Minutoli F, Bottari A, Pergolizzi S, De Renzis C: Treatment of periocular basal cell carcinoma using an advanced stereotactic device. Anticancer Res 34(2): 873-875, 2014.
27 Ferini G, Palmisciano P, Forte S, Viola A, Martorana E, Parisi S, Valenti V, Fichera C, Umana GE, Pergolizzi S: Advanced or metastatic cutaneous squamous cell carcinoma: the current and future role of radiation therapy in the era of immunotherapy. Cancers (Basel) 14(8): 1871, 2022. DOI: 10.3390/cancers14081871
28 Ferini G, Valenti V, Puliafito I, Illari SI, Marchese VA, Borzì GR: Volumetric modulated arc therapy capabilities for treating lower-extremity skin affected by several Merkel cell carcinoma nodules: when technological advances effectively achieve the palliative therapeutic goal while minimising the risk of potential toxicities. Medicina (Kaunas) 57(12): 1379, 2021. DOI: 10.3390/medicina57121379
29 Ferini G, Palmisciano P, Zagardo V, Viola A, Illari SI, Marchese V, Umana GE, Valenti V: Combining a customized immobilization system with an innovative use of the ExacTrac system for precise volumetric modulated arc therapy of challenging forearm sarcomas. Pract Radiat Oncol 13(2): 148-152, 2023. DOI: 10.1016/j.prro.2022.10.005
30 Bertholet J, Mackeprang PH, Mueller S, Guyer G, Loebner HA, Wyss Y, Frei D, Volken W, Elicin O, Aebersold DM, Fix MK, Manser P: Organ-at-risk sparing with dynamic trajectory radiotherapy for head and neck cancer: comparison with volumetric arc therapy on a publicly available library of cases. Radiat Oncol 17(1): 122, 2022. DOI: 10.1186/s13014-022-02092-5
31 Sakamoto Y, Koike N, Takei H, Ohno M, Miwa T, Yoshida K, Shigematsu N, Kishi K: Influence of backscatter radiation on cranial reconstruction implants. Br J Radiol 90(1070): 20150537, 2017. DOI: 10.1259/bjr.20150537
32 Ferini G, Viola A, Valenti V, Tripoli A, Molino L, Marchese VA, Illari SI, Rita Borzì G, Prestifilippo A, Umana GE, Martorana E, Mortellaro G, Ferrera G, Cacciola A, Lillo S, Pontoriero A, Pergolizzi S, Parisi S: Whole Brain Irradiation or Stereotactic RadioSurgery for five or more brain metastases (WHOBI-STER): A prospective comparative study of neurocognitive outcomes, level of autonomy in daily activities and quality of life. Clin Transl Radiat Oncol 32: 52-58, 2021. DOI: 10.1016/j.ctro.2021.11.008